

Laboratory soft x-ray emission due to the Hawking–Unruh effect?

G Brodin^{1,2}, **M Marklund**^{1,2}, **R Bingham**³, **J Collier**⁴, **R G Evans**^{4,5}

1 Department of Physics, Umeå University, SE–901 87 Umeå, Sweden

2 Centre for Fundamental Physics, Rutherford Appleton Laboratory, Chilton, Didcot, Oxon OX11 0QX, U.K.

3 Space Science & Technology Department, Rutherford Appleton Laboratory, Chilton, Didcot, Oxon OX11 0QX, U.K.

4 Central Laser Facility, Rutherford Appleton Laboratory, Chilton, Didcot, Oxon OX11 0QX, U.K.

5 Physics Department, Imperial College, London, U.K

Abstract. The structure of spacetime, quantum field theory, and thermodynamics are all connected through the concepts of the Hawking and Unruh temperatures. The possible detection of the related radiation constitutes a fundamental test of such subtle connections. Here a scheme is presented for the detection of Unruh radiation based on currently available laser systems. By separating the classical radiation from the Unruh-response in frequency space, it is found that the detection of Unruh radiation is possible in terms of soft x-ray photons using current laser-electron beam technology. The experimental constraints are discussed and a proposal for an experimental design is given.

PACS numbers: 04.62.+v, 04.70.Dy

1. Introduction

The discovery that there is a deep connection between black hole physics and seemingly quite different topics, from information theory and statistical mechanics to the search for a quantum theory of gravity, has been highly nontrivial and unexpected. Indeed, it touches upon some of the most important questions in physics today. In this respect, the Hawking radiation [1, 2] is one of the most interesting processes predicted in physics, linking general relativity, quantum field theory and thermodynamics in one single phenomenon [3]. In contrast to classical general relativity, a black hole is predicted to loose energy by thermal radiation with a Hawking temperature

$$T_H = \frac{\hbar g}{2\pi k_B c} \quad (1)$$

where k_B is Boltzmann’s constant, g is the horizon surface gravity, \hbar is Planck’s constant, and c is the speed of light in vacuum. This result tied in naturally to the concept of black hole entropy presented earlier by Bekenstein [4], laying the foundation for black hole thermodynamics. Since the early discoveries of Bekenstein and Hawking numerous papers on black hole thermodynamics have been written, see e.g. Ref. [5] and references therein. Closely related to Hawking radiation is the Unruh-effect [6–8] (also known as the Unruh-Davies-Fulling effect), which predicts that zero-point vacuum fluctuations can be measured as a heat bath of *real particles* by an accelerated particle detector. The temperature of this heat bath is given by the Unruh temperature

$$T_U = \frac{\hbar a}{2\pi k_B c} \quad (2)$$

where a is the proper acceleration of the particle detector. Heuristically, (1) and (2) are related via the equivalence principle, thus the name Hawking–Unruh effect.

For the large black hole masses expected in astrophysics, the Hawking temperature (1) is extremely small, and there is evidently no possibility of ever measuring it. By contrast, several suggestions to measure the Unruh-effect have been made. For example, Bell and Leinaas [9] suggested to look for the Unruh effect in storage rings, Ref. [10] presented the Penning trap as a possible means for detecting the Unruh temperature, Ref. [11] discussed the possibility of using a rapidly changing refractive index for detection of Unruh radiation, and Ref. [12] proposed, based on the concept of analogue gravity, the use of electromagnetic waveguides to simulate the effects of curved spacetime quantum field theory. Although there are numerous works confirming the concept of the Unruh effect [6, 7, 13–15], there is still much controversy surrounding this issue [16–18], thus making it even more important to gain experimental or observational insight into these concepts. For example, Narozhny *et al.* argues that the heat bath is not a universal consequence of acceleration [17]. On the other hand, Ford and O’Connell [18] presents results for a scalar field which supports the concept of a heat bath eventually leading to thermalization at the Unruh temperature for an accelerated system. However, Ford and O’Connell conclude that the system will not emit radiation that can be detected in the laboratory frame, in spite of its finite temperature. For a different opinion concerning the reality of the Hawking–Unruh radiation and further discussions of this issue,

see also Refs. [19, 20]. Assuming that the Unruh-radiation is real, it is clear that a successful detection would be an important milestone. Unfortunately the Unruh-signal is drowned in noise in most of the early proposals. A setup which tries to address this problem has been suggested by Ref. [21], where strong lasers are used to accelerate electrons to ultra-relativistic energies, corresponding to Unruh-temperatures $T_U = 10^4$ K, or higher. While the heat bath felt by the accelerated electrons only contributes with a small correction to the electron motion, the ordinary Larmor radiation has a "blind spot" in the direction of acceleration. Thus the idea was that properly placed detectors may measure radiation produced by electrons responding to the heat bath, without being drowned in the standard Larmor radiation. Similar ideas were put forward in Ref. [22], where modifications due to photon pair correlation and field strengths approaching the Schwinger critical field also were included.

In the present work we propose an experimentally viable method for the detection of the Hawking–Unruh effect using currently available technology. We consider electrons accelerated by lasers in a novel geometric set-up as a means for producing a detectable signal due to the accelerated vacuum temperature. In particular, we chose a configuration with circular electron orbits. This leads to an energy distribution of the vacuum fluctuations, in the electron rest frame, that to some extent deviate from a thermal heat bath. However, the results of for example Ref. [23] for circular motion, shows that an effective temperature of the vacuum fluctuations can still be defined, such that Eq. (2) continues to be a useful approximation. This allows us to calculate the momentum distribution function for the generated non-classical photons. Since a relatively high electron number density is needed for appreciable emission, we include collective effects when comparing with the classical emission. It turns out that the classical power is orders of magnitude larger than the Unruh power, for experimental parameters currently available, a result which is highly problematic in other experimental suggestions. However, here the calculated distribution function shows a clear signature distinguishing Unruh photons from classical photons, in particular giving rise to photons in the soft x-ray regime. We analyse the effects from competing sources, and we conclude that using laser-electron beam systems *currently* in operation it is possible to obtain a clearly detectable signal.

2. Theory

2.1. The Unruh effect in laser fields

We will rely on ultra-intense lasers to accelerate electrons. However, due to the unfavorable scaling with the electron number density n_e , of the amount of radiation produced, we deduce that in a setup with a reasonably high electron density, the classical power will always be much larger than the Unruh-radiation. In order to separate the Unruh-response from the classical radiation we therefore compare their spectral profiles. For this purpose we first note that for presently available field strengths E_0 , we have $E_0 \ll E_{\text{crit}}$, where $E_{\text{crit}} = m^2 c^3 / e \hbar \approx 10^{16}$ V/cm is the Schwinger critical field. Here m is the electron rest mass and e is the elementary charge. From Eq. (2) we thus see that the photon energies of the heat bath will be much smaller than

the electron rest mass. Accordingly, in order to describe the interaction of the electrons with the heat bath, we will view the process as Thomson scattering in the rest frame of the electrons. In essence this means that the detection of the Unruh effect is made by accelerated electrons acting as spherical mirrors of virtual photons, making them real in the laboratory frame. This picture of the process is given further support by the results of Refs. [14, 15], where the analog between moving mirror radiation and Unruh radiation is put on a firm ground.

Introducing the distribution function of thermal photons $f_B(\mathbf{k}, T_U)$, the rate of scattered photons $d\mathcal{N}_s/d\tau$ by a single electron in the rest frame can be written

$$\frac{d\mathcal{N}_s}{d\tau} = \frac{d}{d\tau} \int f_s k^2 d\Omega dk = \sigma_T c \int f_B k^2 d\Omega dk \quad (3)$$

where k is the photon wavenumber, $\sigma_T = e^4/(6\pi\epsilon_0^2 m^2 c^4)$ is the total Thomson scattering cross section, f_s is the distribution function of the scattered photons, and ϵ_0 is the vacuum permittivity and τ is the proper time in the electron rest frame. Next we represent the distribution function as a locally thermal radiation distribution $f_B(\mathbf{k}, T(\mathbf{r}))$ and write the number of scattered photons N_s from a volume V such as

$$\frac{dN_s}{d\tau} = \int_V n_e(\mathbf{r}) \sigma_T c \int f_B(\mathbf{k}, T(\mathbf{r})) k^2 d\Omega dk dV \quad (4)$$

where n_e is the number density of electrons. Hence the scattered distribution function evolves according to $df_s/d\tau = \sigma_T c f_B$. Next we assume that the volume is sufficiently small, such that for a given time the spatial dependence of the electron velocity is negligible within V (i.e. we only count the contribution from the central part of the laser pulse). The power from the Unruh effect $P_{U,\text{rest}}$ emitted in the electron rest frame then reads

$$P_{U,\text{rest}} = \frac{d}{d\tau} \int_V \int \hbar \omega_{\text{rest}} f_s(\mathbf{k}) k^2 d\Omega dk dV \quad (5)$$

where ω_{rest} is the photon frequency in the rest frame. In order to evaluate the power $P_{U,\text{lab}}$ emitted in the laboratory frame, we introduce spherical coordinates, with the z -axis perpendicular to the velocity, and we write $\omega_{\text{lab}} = \omega_{\text{rest}} \gamma(v) [1 - (v/c) \sin \theta \cos(\phi - \phi_v)]$, where ω_{lab} is the photon frequency in the lab-frame and ϕ_v is the angle between the velocity and the x -axis. Using the analogy between moving mirror radiation and the Unruh effect [14, 15], the emitted laboratory power is then calculated as

$$P_{U,\text{lab}} = \int_V \int \hbar \omega_{\text{lab}} \frac{df_s}{d\tau} \frac{d\tau}{dt} k^2 d\Omega dk dV = P_{U,\text{rest}} \quad (6)$$

where the last step comes from noting that f_s and the phase space volume element are scalars.

Next, we want to compare the radiation generated due to the Unruh effect with the classical emission. As a model, we consider electrons accelerated by counter propagating laser pulses with left and right hand circular polarization. The advantage with circular polarization is twofold. Firstly, due to the high symmetry, a simple harmonic current response with circular orbits solves the fluid equations of motion [24], and thus the electron response is more easily evaluated. Secondly, collective nonlinear effects (e.g. harmonic generation, induced density fluctuations, etc., see Ref. [25] for a list of possible mechanisms) that may induce classical competing high-frequency emission is thereby minimized.

The electric field can then be written $\mathbf{E} = E_0 [\exp i(k_0 z - \omega_0 t) + i(-k_0 z - \omega_0 t)] \hat{\mathbf{x}}/2 + E_0 [\exp i(k_0 z - \omega_0 t) + i(-k_0 z - \omega_0 t)] \hat{\mathbf{y}}/2 + \text{c.c.}$, where c.c. stands for complex conjugate and ω_0 and k_0 are the laser frequency and wavenumber, respectively. We note that in a region $|z| \ll \lambda_L$, where λ_L is the laser wavelength, the corresponding magnetic field is vanishingly small for all times. Concentrating on this region, the electron velocities can be written as

$$\mathbf{v} = \frac{eE_0 [\cos(\omega_0 t) \hat{\mathbf{x}} + \sin(\omega_0 t) \hat{\mathbf{y}}]}{m\omega_0 \sqrt{1 + (eE_0/m\omega_0 c)^2}} \quad (7)$$

The Unruh emission is described by the scattered distribution function $f_s(\mathbf{k})$, which is shown in Fig. 1 for $\gamma = 70$. We note the strong beaming in the direction of the velocity. We deduce from Eqs. (3)–(5) and (7) that the energy distribution due to the Unruh effect in the laboratory frame, averaged over a period time, will be (approximately) thermal with a temperature

$$T_{\text{lab}} = \frac{\gamma e \hbar E_0}{2\pi k c m} \quad (8)$$

in spite of the strong anisotropy of f_s . The high temperature means that the characteristic wavelength in the laboratory frame typically will be much shorter than the laboratory orbit radius, a result which will be helpful in separating the Unruh radiation from the classical radiation. Here it should be noted that in the case that the particle deviates from stationary orbits, the asymptotic part of the spectra will follow a power law, rather than being thermal, as deduced in Ref. [26]. Since, such deviations are inevitable, the highest frequencies will certainly not be thermally distributed. Our detection scheme, however, is based on detection of the central part of the frequencies. Thus a small deviation from stationarity is of limited importance in our case. Here we also neglect the effect that the photons in the heat bath are created in pairs. Note, however, that a proposal that attempts to use this fact, measuring the correlation between individual scattering events, has recently been proposed [22].

Next evaluating the radiated Unruh power using Eqs. (3)–(5) we obtain

$$P_{U,\text{lab}} = \frac{N e^8 E_0^4 \hbar}{1440 \pi^3 c^{10} m^6 \epsilon_0^2} \quad (9)$$

We note that even for the highest laser fields currently available, $E_0 \sim 2 \times 10^{12}$ V/cm, we still need a large number of accelerated electrons (at least $N > 10^8$) to reach detectable levels of the Unruh radiation.

2.2. Spectral structure

Let us now study the spectral properties of the radiation. For an irradiance of $10^{21} - 10^{22}$ W/cm², we note that the characteristic energy of the Unruh photons [cf. (8)] is larger than the laser photon energies, by several orders of magnitude, assuming the laser works in the optical range. Thus the assumption to view the periodic variation of the laser field as slow when considering the spectral properties of the Unruh radiation is justified. Furthermore, within the framework of our model, the spectral properties of the classical emission is suppressed for a wide range of frequencies (see Sec. 3), and thus it is straightforward to

separate the two contributions. However, we note that we will only get a few photons due to the Hawking–Unruh effect per laser shot, even for a rather high electron number density, $n_e = 10^{21} \text{ cm}^{-3}$. Combining Eqs. (8)–(9) we can write the number of photons per shot as

$$N_U = 0.084 \left(\frac{E_p}{15 \text{ J}} \right)^2 \left(\frac{0.5 \times 10^{15} \text{ W}}{P} \right) \left(\frac{800 \text{ nm}}{\lambda_L} \right) \left(\frac{n_e}{10^{21} \text{ cm}^{-3}} \right), \quad (10)$$

where E_p is the pulse energy for each pulse, P is the laser power, λ_L is the laser wavelength and n_e is the electron density. Similarly, the characteristic photon energy can be written as

$$\hbar\omega_{\text{char}} = 582 \left(\frac{I}{10^{22} \text{ W cm}^{-2}} \right) \left(\frac{\lambda_L}{800 \text{ nm}} \right), \quad (11)$$

where I is the intensity and $\hbar\omega_{\text{char}}$ is given in units of eV. In Fig. 2 a schematic view of the experimental set-up is given. Two opposed focused laser beams with opposite circular polarization are allowed to interact with an under-dense laser produced electron beam, with a drift velocity well below c . The soft x-ray photons due to the Hawking–Unruh effect are emitted in a narrow band perpendicular to the incoming laser beams. Careful placement of the photon detectors leads to a nearly full x-ray coverage. The output when varying the intensity in a number of different laser systems (for which the necessary numbers are given in Table 1) is shown in Fig. 3.

3. Classical radiation

Next we study the vector potential due to the classical emission, that can be written $\mu_0 \int (\mathbf{J}(t_{\text{ret}}, |\mathbf{r} - \mathbf{r}'|)/r) dV'$, in the radiation zone, where t_{ret} is the retarded time. A major difficulty for detecting the Unruh contribution is that the Larmor (or synchrotron) radiation power (described by the single particle delta function contributions to the retarded current) is always much larger than the Unruh response for all frequency regimes. These arguments apply if we consider the radiation from a single particle. When increasing the particle density, the Unruh radiation power (9) scales linearly with the number of particles, but the classical radiation may grow equally fast or even faster. Fortunately, different parts of the classical spectrum behave differently, depending on whether the emitted radiation is a collective fluid effect, or a single particle effect. If we look on the shortest emitted wavelengths, neighbouring particles are typically much more than a wavelength away, and we cannot detect interference effects in the radiation pattern. As a consequence, the classical radiation scales linearly with the number of particles, and it will be extremely difficult to see the Unruh response in the emitted radiation for such wavelengths, since the gyrating motion of the electrons produces synchrotron radiation at harmonics of the laser frequency up to the frequencies of the order $\sim \gamma^3 \omega_0$. In principle, for strictly periodic motion the synchrotron radiation is built up of multiples of the laser frequency, but a finite bandwidth of the laser will limit our possibility to benefit from this. However, studying radiation with wavelengths much longer than the nearest neighbour distance of the particles is more useful. For the electron densities considered, $n_e = 10^{21} \text{ cm}^{-3}$, wavelengths of the order $\lambda = 0.01 \mu\text{m}$ could be suitable, fulfilling $\lambda \ll L_{mn}$, where L_{mn} is the nearest neighbour distance. For such wavelengths, the single particle

radiation is suppressed[‡] and the output from the gyrating motion can be described with a fluid model. Assuming that the current density decays smoothly with the radius, and using Eq. (7) the classical radiated power becomes $P_{\text{classical}} = \eta N^2 e^4 E_0^2 / m^2 c^3 \gamma^2$ where $N = n_e 2\pi R^2 L$ is the number of electrons in a pulse with length $2L$ and radius R , and η is a geometrical factor of order unity. This collective fluid response is the main source of classical emission, but its frequency spectrum is determined by the laser frequency, and thus it is limited to the optical range.

The result that the output is negligible for frequencies deviating from the fundamental frequency depends on two facts. Firstly, the time-dependence of the current density in each volume element should be quasi-monochromatic such that we can write $\mu_0 \int_{V'} \mathbf{J}(t_{\text{ret}}, |\mathbf{r} - \mathbf{r}'|/c) dV' = \exp[-i\omega(t - r/c)] \mu_0 \int_{V'} \exp(i\omega \mathbf{r} \cdot \mathbf{r}'/cr^2) \mathbf{J}_s(|\mathbf{r} - \mathbf{r}'|) dV'$ in the radiation zone, where $\mathbf{J}_s(|\mathbf{r} - \mathbf{r}'|)$ contains the spatial dependence of the current density. Secondly, in order to suppress synchrotron radiation effects, the volume V' where the current density \mathbf{J}_s is non-zero *must not* be strongly time-dependent. This later condition is fulfilled if the radial dependence of the pulse electric field smoothly approaches zero outside the central pulse region, in which case the weak time-dependence of the interaction volume also makes the expression $\int_{V'} \exp(i\omega \mathbf{r} \cdot \mathbf{r}'/cr^2) \mathbf{J}_s(|\mathbf{r} - \mathbf{r}'|) dV'$ time-independent. As a consequence the higher frequencies of the classical spectra is suppressed up to the wavelengths where the fluid model breaks down. Thus, there is a window of detectable wavelengths, shorter than the laser wavelength, but much longer than the inter particle distance. The parameters of an experiment can be chosen to fit the Unruh radiation into this window.

Table 1. The relevant parameter values for different two-beam laser systems. In the first column the each laser pulse energy is given, in the second the pulse power, in the third the pulse focal intensity, and in the fourth the laser wavelength. The Ti:Sapphire is assumed to have standard high-intensity properties, the Astra–Gemini system is in operation (from 2007) at the Rutherford Appleton Laboratory (RAL) in the U.K., with a proposed upgrade, the Vulcan laser is in operation at the RAL, and the Omega EP laser will be operational in Rochester (USA). The HiPER (High Power Experimental Research Facility) and ELI (Extreme Light Infrastructure) are European infrastructure projects under planning [30, 31].

Laser type	Energy (J)	Power (PW)	Intensity (W/cm ²)	Wavelength (nm)
Ti:Sapphire	1	0.03	10^{21}	800
Astra–Gemini	15	0.5	10^{22}	800
AG upgrade	15	0.5	$\leq 10^{24}$	800
Vulcan	250	0.5	5×10^{20}	1054
Omega EP	≥ 2500	0.25	6×10^{20}	1054
HiPER 1	4500	150	5×10^{24}	1054
HiPER 2, ELI	37500	2500	5×10^{26}	1054

[‡] The power of single particle radiation scales as $1/N$, where N is the number of electrons (this result is obtained from a random walk model, in which the contribution to the vector potential from each particle has a random phase compared to the others). However, when the wavelength of the radiation is much longer than the nearest neighbor distance, the uncertainty of the phase of the contribution from each accelerated electron is much less than $\pi/2$, and the single particle radiation is thereby suppressed.

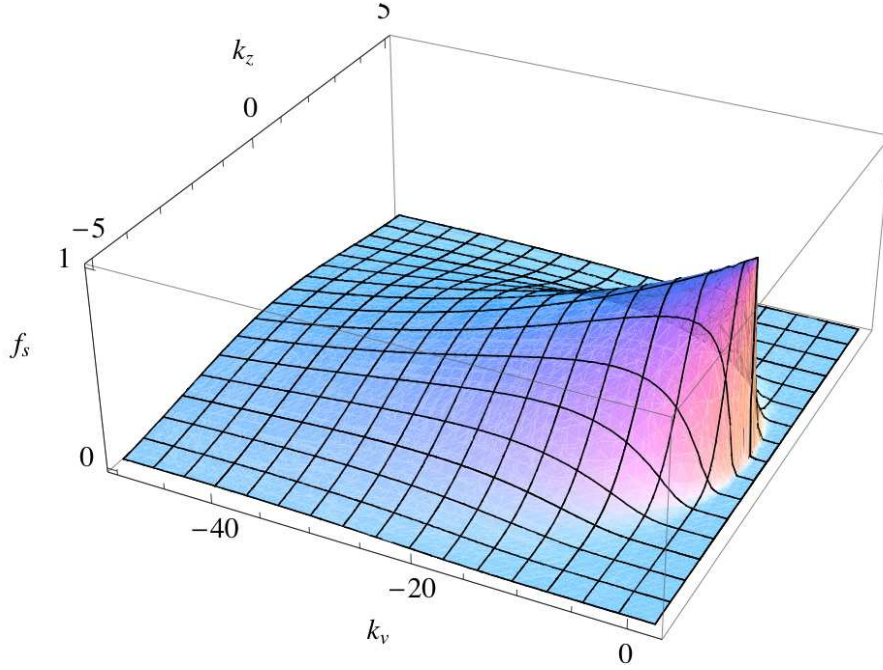


Figure 1. A cross section of the normalized scattered distribution function $f_s(k_v, k_z)/f_s(0, 0)$ as a function of normalized wavenumbers ($\hbar k_v/k_B T_U \rightarrow k_v$ and $\hbar k_z/k_B T_U \rightarrow k_z$). Here k_v denotes the wavenumber in the direction of the velocity. The figure corresponds to $\gamma \approx 70$, and the cross-section is shown for $k_\perp = 0$, where k_\perp is the component perpendicular to k_v and k_z . We see that there is a strong beaming effect in the direction of the velocity.

Other mechanisms that could generate radiation competing with the Unruh contribution includes particle collisions. To avoid this source, we consider a laser produced electron beam, rather than a plasma, in order to prevent the high energy electrons to scatter of ions and produce competing soft x-rays. Moreover, we note that efficient absorption of laser energy with subsequent x-ray generation [27] due to electron-electron collisions can be avoided if the density is kept undercritical. This is consistent with an electron beam density $n_e \sim 10^{21} \text{ cm}^{-3}$, in which case the synchrotron emission is suppressed for photon energies up to 1 KeV. This leads to an optimal irradiance in the range $\sim 10^{21} - 10^{22} \text{ W/cm}^2$. Specifically, for a pulse energy of 3kJ, a focused intensity of 10^{21} W/cm^2 , and a wavelength of $1 \mu\text{m}$ together with an electron density 10^{21} cm^{-3} we generate more than 2×10^3 Unruh photons/shot, with an energy of the order of 100eV . Naturally, the next generation of laser facilities in the early planning stage, like ELI or HiPER would produce even more impressive results. It should be stressed, however, that our experiment does not benefit from the huge focusing capabilities in those cases, since very high intensities move the characteristic photon energy outside the window where classical emission is suppressed. Nevertheless, in case a proper degree of focusing is chosen, naturally the large pulse energies in facilities like HiPER 2 or ELI (see table 1) make them excellent choices for our suggested experiment. In conclusion, we find that classical soft x-ray emissions can be sufficiently suppressed in the relevant parameter regime.

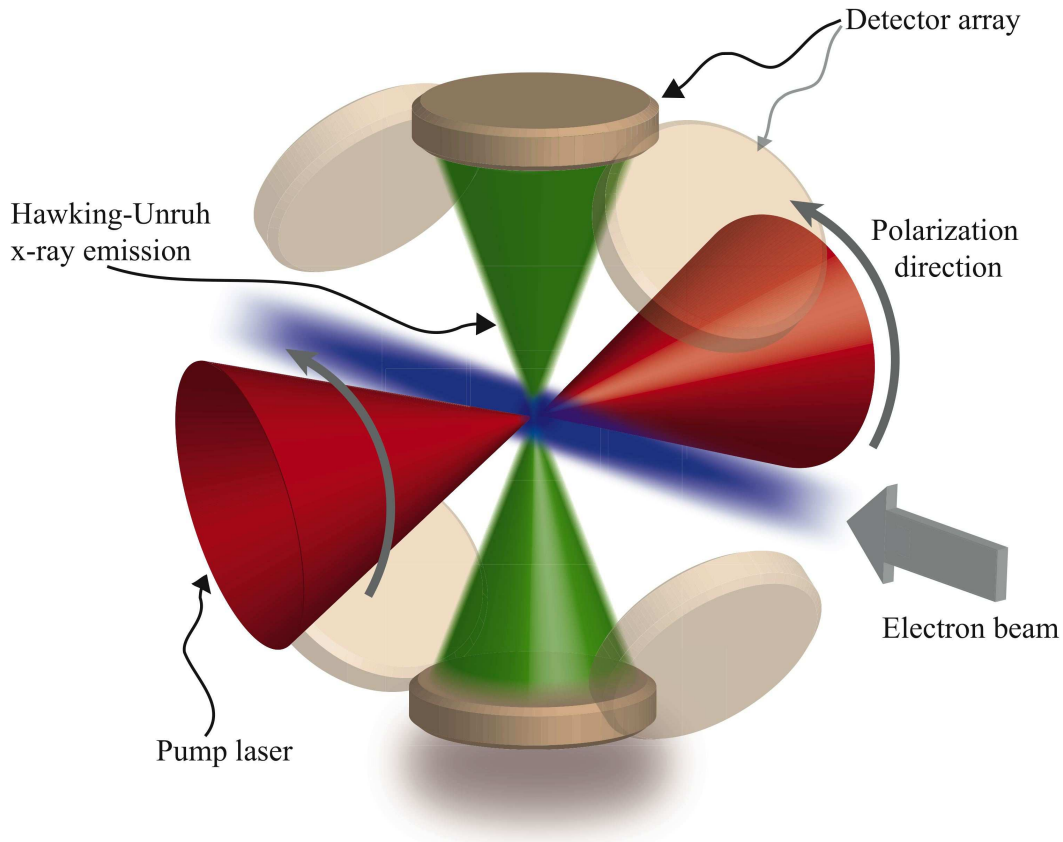


Figure 2. A schematic view of the setup. The emitted radiation will be sharply beamed in the direction of the electron velocity. Thus the detectors only have to cover a short distance in the direction of propagation

4. Conclusion and discussion

An unambiguous detection of the Hawking–Unruh effect would be an important breakthrough, shedding light on the deep and fundamental connection between general relativity, quantum field theory, and thermodynamics and settling much of the controversies that have arisen over the subject, see e.g. Refs. [17–20]. The details of the possible signals detected through such experiments could even have interesting consequences for a future quantum theory of gravity [28, 29]. Noting the similarity with radiation from moving mirrors [13–15], we have calculated the distribution function for the photons generated from laser accelerated electrons, due to the Unruh effect. The reader might ask whether the analogy between infinitely heavy mirrors and finite mass electrons is valid or not. After all, it is the finite mass of the electrons that allow them to respond to the heat bath. However, we stress that when determining the cross-section of the electron “mirrors”, the finite electron mass is incorporated. Moreover, Chen & Tajima [21] suggested a novel means to detect the Unruh effect through single electron dynamics. However, in practice a large electron density is needed, making collective effects essential. In particular, the competing classical radiation scales as N^2 , while the Unruh radiation scales as N , where N is the number of electrons

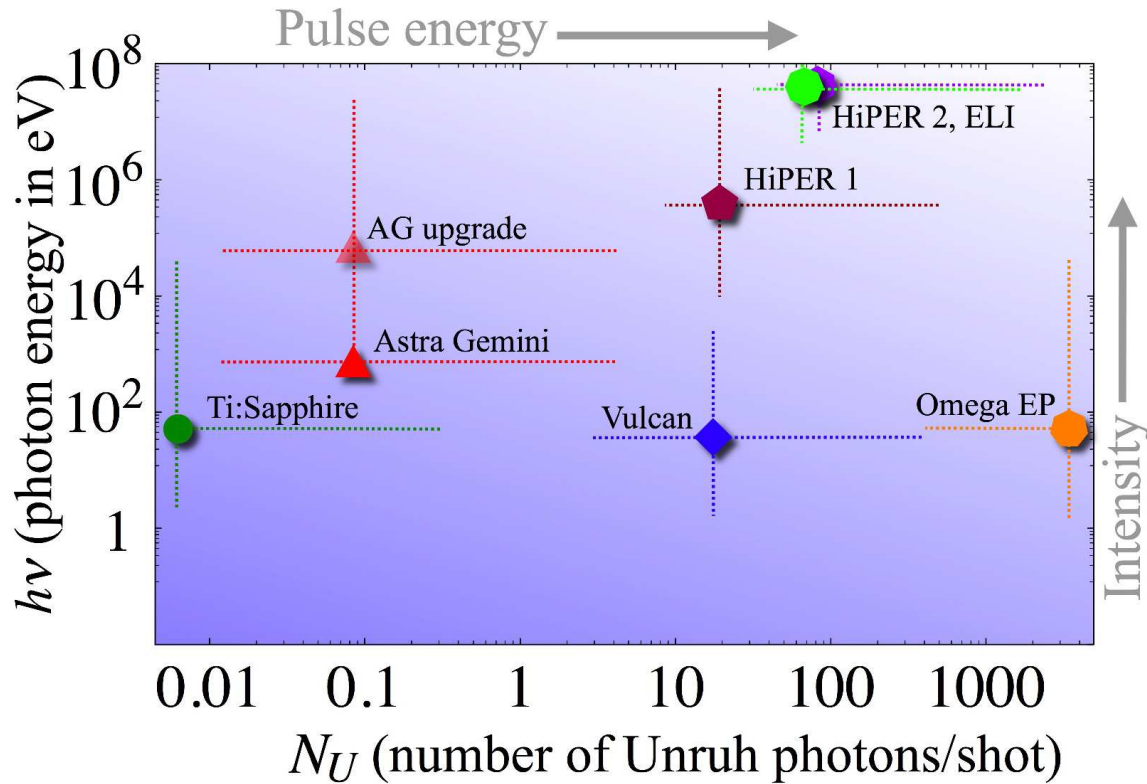


Figure 3. The figure shows the characteristic energy $\hbar\omega_{\text{char}}$ in units of eV of the photons generated due to the Unruh effect and its relation to the number of photons N_U per shot for different ultra-intense laser systems. The horizontal lines correspond to variations in pulse energy (pulse length), keeping the focused intensity constant. The vertical lines correspond to variations in intensity, keeping the pulse length and pulse energy constant. The different values are computed using the same electron number density $n_e = 10^{21} \text{ cm}^{-3}$. The relevant parameter values can be found in Table 1.

in the interaction region. Thus, the effective spatial window in the Larmor radiation scales as $1/N$ ($\sim 10^{-9}$ for an electron density of 10^{21} cm^{-3} and a spot-size of the order of μm), making spatial filtering insufficient. Instead, one needs to include the collective properties of the classical radiation, when comparing the classical and Unruh *spectral* distributions. For the spectral signature of the Unruh photons to be distinguishable from competing effects, the classical soft x-ray emission must be eliminated. The key in doing this is to consider a pure electron plasma to avoid electron-ion scattering, and to limit the heating of the laser target, which can be achieved by keeping the electron density well below the critical density [27]. For an electron beam density $n_e \sim 10^{21} \text{ cm}^{-3}$ the classical synchrotron emission is suppressed up to photon energies of 1 keV due to destructive interference, which means that the spectral properties of the Unruh radiation is ideal for detection for an irradiance of the order $10^{21} - 10^{22} \text{ W/cm}^2$. In conclusion, we have shown that, through proper experimental design, detection of the Unruh effect using accelerated electron is possible with currently available technology.

Acknowledgements

This research was supported by the Swedish Research Council and the Centre for Fundamental Physics, Rutherford Appleton Laboratory, U.K.

References

- [1] Hawking S W 1974 *Nature* **248** 30
- [2] Hawking S W 1975 *Commun. Math. Phys.* **43** 199
- [3] Susskind L 2006 *Nature Physics* **2** 665
- [4] Bekenstein J D 1973 *Phys. Rev. D* **7** 2333
- [5] Wald R M 2001 *Living Rev. Relativity* **4** 6
- [6] Davies P C W 1975 *J. Phys. A: Math Gen.* **8** 609
- [7] Unruh W G 1976 *Phys. Rev. D* **14** 870
- [8] Davies P C W and Fulling S A 1977 *Proc. R. Soc. A* **354** 529
- [9] Bell J S and Leinaas J M 1987 *Nucl. Phys. B* **284** 488
- [10] Rogers J 1988 *Phys. Rev. Lett.* **61** 2113
- [11] Yablonovitch E 1989 *Phys. Rev. Lett.* **62** 1742
- [12] Schützhold R and Unruh W G 2005 *Phys. Rev. Lett.* **95** 031301
- [13] Davies P C W 2005 *J. Opt. B: Quantum Semiclass Opt.* **7** S40
- [14] Obadia N and Parentani R 2003 *Phys. Rev. D* **67** 024021
- [15] Obadia N and Parentani R 2003 *Phys. Rev. D* **67** 024022
- [16] Grove P G 1986 *Class. Quantum Grav.* **3** 802
- [17] Narozhny N B *et al.* 2004 *Phys. Rev. D* **70** 048702
- [18] Ford G W and O’Connell R F 2006 *Phys. Lett A* **350** 17
- [19] Unruh W G 1992 *Phys. Rev. D* **46** 3271
- [20] Fulling S A and Unruh W G *Phys. Rev. D* **70** 048701
- [21] Chen P and Tajima T 1999 *Phys. Rev. Lett.* **83** 256
- [22] Schützhold R, Schaller G and Habs D 2006 *Phys. Rev. Lett.* **97** 121302
- [23] Korsbakken J I and Leinaas J M 2006 *Phys. Rev. D* **70** 084016
- [24] L. Stenflo, 1976 *Phys. Scripta*, **14**, 320.
- [25] P.K. Shukla, N.N. Rao, M.Y. Yu and N.L. Tsintsadze, 1986 *Physics Reports*, **138**, 1.
- [26] N. Obadia and M. Milgrom, 2007, *Phys. Rev. D* **75**, 065006
- [27] Skobelev I Yu *et al.* 2002 *Zh. Exsp. Teor. Fiz.* **121** 188
- [28] Ling Y, Hu B and Li X 2006 *Phys. Rev. D* **73** 087702
- [29] Amelino-Camelia G, Arzano M, Ling Y and Mandanici G 2006 *Class. Quantum Grav.* **23** 2585
- [30] Dunne M 2006 *Nature Physics* **2** 2
- [31] Gerstner E 2007 *Nature* **446** 16